

**NASA CONTRACTOR
REPORT**

NASA CR-384



NASA CR-384

0099604



**FLEXURAL VIBRATIONS OF
CONICAL SHELLS WITH
FREE EDGES**

by W. C. L. Hu, J. F. Gormley, and U. S. Lindholm

Prepared under Contract No. NASr-94(06) by
SOUTHWEST RESEARCH INSTITUTE
San Antonio, Texas
for

NATIONAL AERONAUTICS AND SPACE ADMINISTRATION • WASHINGTON, D. C. • MARCH 1966



FLEXURAL VIBRATIONS OF CONICAL SHELLS WITH FREE EDGES

By W. C. L. Hu, J. F. Gormley, and U. S. Lindholm

Distribution of this report is provided in the interest of information exchange. Responsibility for the contents resides in the author or organization that prepared it.

Prepared under Contract No. NASr-94(06) by
SOUTHWEST RESEARCH INSTITUTE
San Antonio, Texas

for

NATIONAL AERONAUTICS AND SPACE ADMINISTRATION

SUMMARY

Experimental data is presented for the resonant frequencies and associated mode shapes of truncated conical shells with free edges in transverse vibration. A wide range of the geometrical and modal parameters is covered. A semi-empirical frequency equation is developed which can be used to predict the first axial mode resonances with satisfactory accuracy.

NOMENCLATURE

a, b	radius of the major and minor base, respectively
E	Young's modulus
h	thickness of shell
m	modal parameter, associated with meridional mode shape.
n	circumferential wave number
s	distance along meridian, measured from apex
t	time
u, v, w	displacement components, in meridional, circumferential, and normal directions, respectively
α	semivertex angle
ϵ	$= h^2/12a^2$, thickness parameter
θ	circumferential coordinate angle
ν	Poisson's ratio
ρ	mass density
ω	natural frequency in rad/sec
Ω	$= \omega a \sqrt{\rho/E(1-\nu^2)}$ dimensionless frequency parameter

INTRODUCTION

The vibrational characteristics of thin conical shells have received increased attention in recent years because of their extensive applications in space vehicles and other structures. In a current research program on shell dynamics, a comprehensive investigation has been made on vibrations of freely supported conical shells, and the correlative analytical and experimental results obtained therefrom have been reported in Ref. 1. As a part of the study of the boundary condition effects, further experiments were extended to the case of truncated conical shells with free edges. The present paper presents the measured resonant frequencies and associated mode shapes of free-free conical shells over a fairly complete range of geometrical and modal parameters.

Like the free-free cylindrical shell, thin conical shells with free edges are developable surfaces, and possess very small rigidity to transverse motion (Rayleigh's inextensional deformations). Therefore, the lowest family of natural frequencies, associated with flexural modes, is extremely small compared to the higher families in the spectrum. This flexibility and the low frequencies cause particular difficulties both in experiments and in analytical calculations. In the experimental procedure, special care must be paid to keep the highly unstable, vibrating shell model in a steady-state motion, and to separate different normal modes with extremely close frequencies. In analysis,

the low frequency was found to make the governing eigenvalue problem nearly singular, thus requiring a high-precision calculation procedure.

Careful analysis of the resonant frequency data shows, however, that the natural frequencies of the first axial modes of free-free conical shells differ only slightly from those predicted by the inextensional theory of cylindrical shell vibrations. An empirical modification term, taking account of the conical angle, was found sufficient to give satisfactory accuracy over the entire range of parameters studied.

EXPERIMENTAL APPARATUS AND PROCEDURE

The apparatus and procedure used to excite and record the resonant frequencies and to map the mode shape are the same as described in Ref. 1. The steel shell models are driven by pulsed magnetic fields through two symmetrically located magnets, and the transverse displacement response is measured by a non-contacting probe; thus neither the excitation nor the measuring device alters the vibrational characteristics of the thin shell appreciably. A photograph of the experimental set-up is shown in Fig. 1.

Four shell models were formed from 0.010 inch thick rolled steel shim stock. The cones were developed from flat sheets and butt-welded along a generator, with negligible discontinuity introduced by the joint. The geometry of the cones is described in Table 1.

TABLE 1

<u>Model No.</u>	<u>α</u>	<u>s_2/s_1</u>	<u>h/a</u>	<u>$a(\text{in.})$</u>
1	14.2°	2.23	0.00166	6.07
2	30.2°	2.27	0.00127	7.95
3	45.1°	2.25	0.00112	8.96
4	60.5°	2.25	0.00101	10.00

To simulate the free-edge boundary condition, the conical shell model was placed with its minor edge on three equally spaced, soft,

foamed-rubber cushions, cut in small cylinders of $1/2$ inch diameter (Fig. 1). The cushions were very flexible and had only negligible local effect on the shell motion. The reason of supporting the cone on its minor edge is that, from experimental evidence, the normal mode vibrations under consideration are usually characterized by the pre-dominate transverse motion near the major edge, with only small displacements at the minor edge. Therefore, any constraint at the major edge would result in a relatively larger distortion of the mode shape.

There are special difficulties arising in the excitation of free-free conical shells, mainly because of their low rigidity. The d.c. component of the exciting magnets was found strong enough to distort somewhat the circular shape, and considerable care had to be taken to keep the shell model from being attracted to the magnets; hence low excitation forces were used to maintain a steady motion. Stray wind currents were also found sometimes to rock the model on its supports, but their effect was removed from the mode shape plots by a band-pass frequency filter. The inevitable slight deviation from a perfect circular shape also caused difficulties in mapping the circumferential mode shape. The nodal lines and nodal circles were not always clearly marked by a zero displacement line, but had to be determined by observing the phase shift of the displacement signal as the probe crossed a nodal line. The band-pass frequency filter also removed other impurities in the displacement signals.

RESULTS AND DISCUSSION

Resonant Frequencies

The resonant frequencies for the free-free cones are presented graphically in Figs. 2 through 5 for the four shell models tested. The non-dimensional frequency parameter Ω is plotted against the circumferential wave number n .

It is seen that, for the first axial mode number ($m = 1$), the resonant frequencies form a smooth curve, essentially parabolic in shape. The lowest natural frequency always occurs at $m = 1$ and $n = 2$. The higher axial modes ($m = 2$ and 3) exhibit a more complex tendency. For example, the curves corresponding to $m = 2$ have an abrupt change in slope at values of n between 6 and 10, which, as will be seen later, is connected to an unusual change in the axial mode shape with increasing n . The high density of the natural frequencies is obvious from the frequency plots.

As mentioned before, the resonant frequencies of free-free conical shells are slightly higher than those predicted by the inextensional frequency equation for a cylindrical shell. From Ref. 3, the frequency equation for inextensional modes of a long, free-free cylinder has the simple form

$$\Omega = \sqrt{\epsilon} \frac{n(n^2-1)}{\sqrt{n^2+1}} \quad (1)$$

where $\epsilon = h^2/12a^2$ is the thickness parameter. By comparing the measured frequencies of the four conical shell models with the corresponding values given by Eq. (1), it was found that a modification term proportional to $\sin(3\alpha/2)$ was needed to account for the increased stiffness due to the taper. Thus, the following semi-empirical frequency equation is proposed for thin conical shells:

$$\Omega = \sqrt{\epsilon} \frac{n(n-1)}{\sqrt{n^2+1}} (n+1 + 4 \sin \frac{3\alpha}{2}) \quad (2)$$

The frequencies calculated according to Eq. (2) are also plotted vs n in Figs. 2 through 5 as solid curves. It is seen that the agreement is in general excellent for the whole range of parameters tested, with the exception that, at low values of n , say $n = 2$ and 3 , the relative errors are appreciable due to the low numerical values of the frequencies themselves.

Since relatively little experimental data have been published pertaining to the vibrations of free-free conical shells, the range of applicability of Eq. (2) with regard to the completeness parameter s_2/s_1 is uncertain. Recent work of Watkins and Clary (Ref. 2) contains experimental data for free-free cones with s_2/s_1 ranging from 1.16 to 2.33, the latter value being approximately the same as in the present experiments. A comparison of their measured resonant frequencies and those calculated by Eq. (2) is given in Fig. 6, where n is the circumferential wave number at the major edge, since in Ref. 2,

different n values were observed at the minor edge*. It is seen that the agreement is also good, indicating that the natural frequencies of free-free conical shells are not sensitive to changes in the completeness parameter s_2/s_1 . The mode shapes in general show relatively little motion at the small end of the cone, so the completeness parameter (s_2/s_1) would not be expected to affect the frequency greatly.

Mode Shapes

Experimental mode shapes of selected modes were mapped for the four cone models described in Table 1. The mode shapes for the four cones were similar, so only the results for the 45° cone will be discussed in detail. The circumferential mode shapes were found to be simply proportional to $\sin n\theta$, as predicted by theory. Figures 7 and 8 show the normalized transverse mode shapes along a generator for $m = 1$ and 2 respectively. In Fig. 7 the transverse displacement is seen to be essentially linear for $n = 2$ to 10, as assumed by Rayleigh's inextensional theory. The nodal circle is near the small end of the cone at low n , but slowly shifts toward the middle as n increases. However, as n increases from 10 to 12, a drastic change in the mode shape occurs. It is seen that the generator abruptly changes from the nearly straight form (inextensional deformation) to a curved form with decreased motion near the smaller end.

* See discussion given in Ref. 4.

In Fig. 8, similar mapping of mode shapes is shown for $m = 2$. It is interesting to note that the number of nodal circles does not accordingly increase to two as might be expected. The mode shapes in general resemble those for $m = 1$, except that the nodal circles all shift toward the major end. A transition can also be observed at $n = 10$ to 12 , where the generator begins to deviate from a nearly straight line and bend into a reverse curve. This transition is reflected on the frequency plots (Fig. 4) where it can be seen that the slope of the Ω - n curve suddenly decreases. This indicates that the new mode pattern formed from this transition has a slightly lower energy level than the corresponding inextensional modes.

CONCLUSIONS

The natural frequencies of four conical shell models have been measured for the free-edge boundary condition, with normal displacement mode shapes of selected modes mapped along a generator. The density of the frequency spectrum was found extremely high. For a conical shell with given geometry, it is highly probable that several normal modes, with different values of modal parameters m and n , may have the same or very close frequency; thus, complex response patterns are likely to take place for excitation at any forcing frequency.

A semi-empirical frequency formula is proposed which predicts the frequencies of the first axial mode ($m = 1$) with good accuracy. From the measured mode shapes, it can be justifiably concluded that, if n is not too large, (say, $n \leq 10$ for the shell models tested), the first axial modes assume the inextensional deformation.

Finally, it may be remarked that, for thin, free-free conical shells, the flexural frequencies are directly proportional to the thickness ratio h/a , and are insensitive to a change in the completeness parameter.

REFERENCES

1. Lindholm, U.S. and Hu, W.C.L., "Nonsymmetric Transverse Vibrations of Truncated Conical Shells," Proc. of AIAA Symposium on Structural Dynamics and Aeroelasticity, Boston, Mass., August 30-September 1, 1965.
2. Watkins, J.D. and Clary, R.R., "Vibrational Characteristics of Thin-Wall Conical Frustum Shells," AIAA Journal, 2, 10, pp. 1815-1816, (1964).
3. Rayleigh, THEORY OF SOUND, 2nd Edition, Dover, New York, pp. 384-386, (1945).
4. Hu, W.C.L., "Comments of 'Vibrational Characteristics of Thin-Wall Conical Frustum Shells,'" AIAA Journal, 3, p. 1213, (1965).

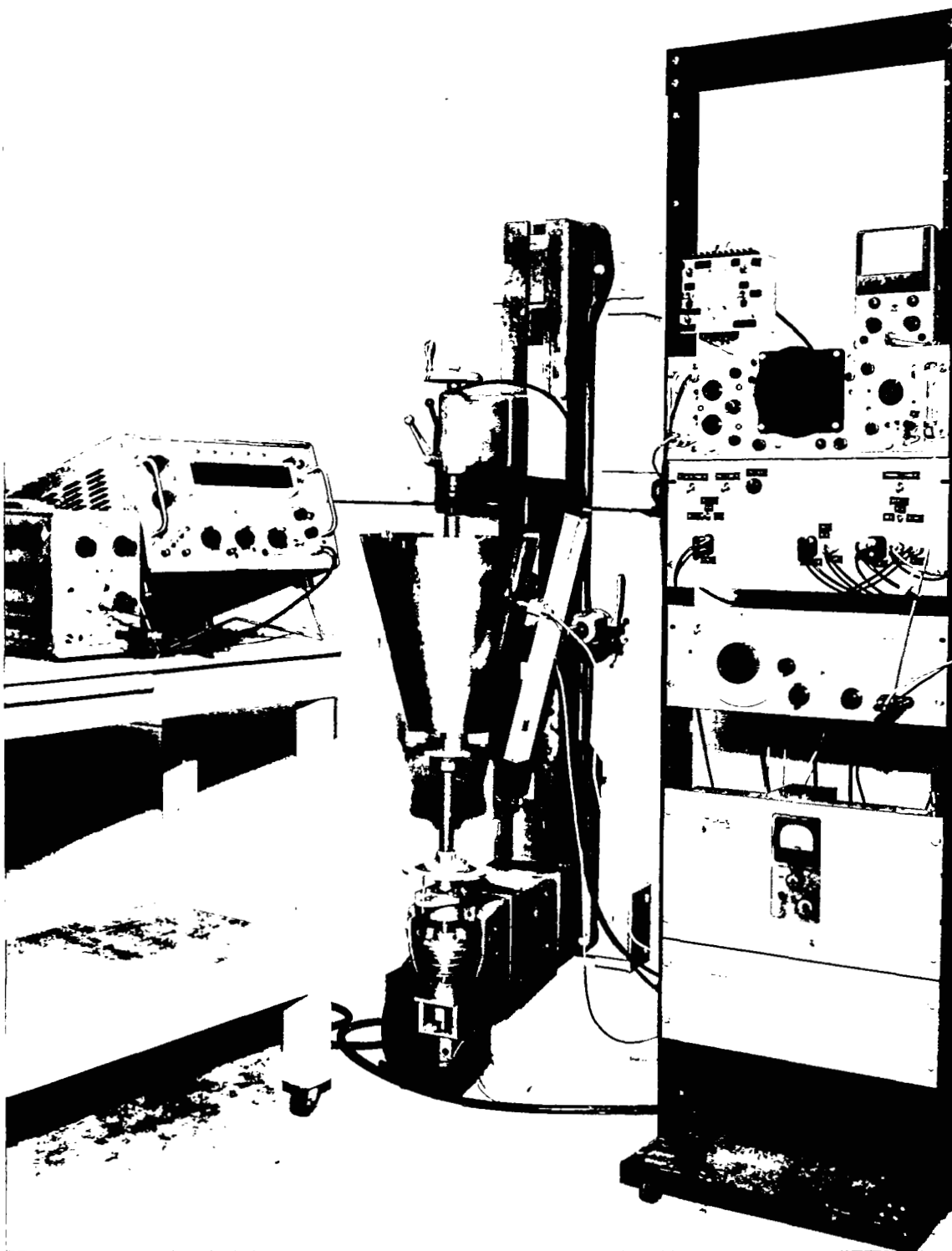


FIGURE 1. EXPERIMENTAL SET-UP

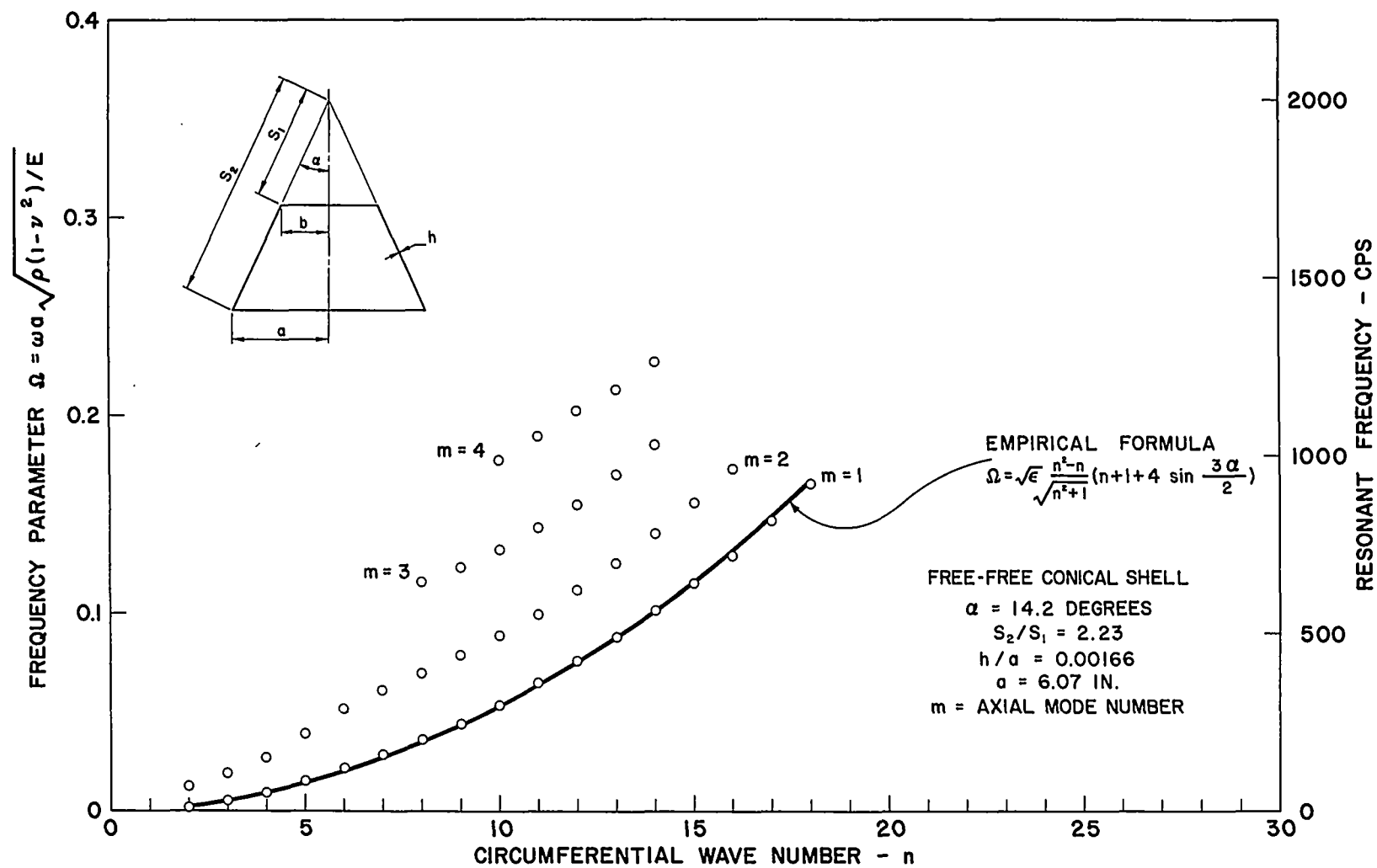


Figure 2. Resonant Frequencies for 14.2° Cone

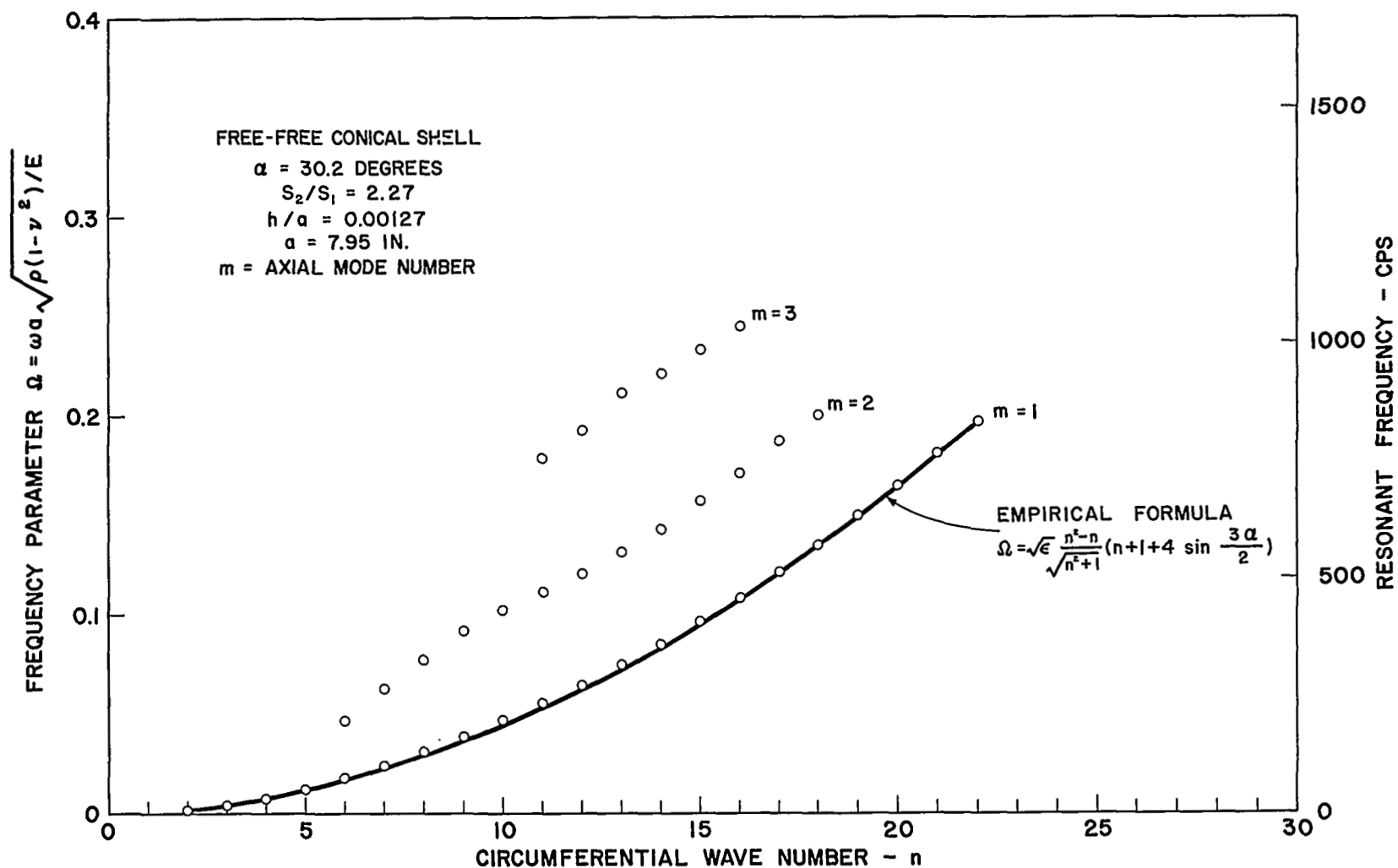


Figure 3. Resonant Frequencies for 30.2° Cone

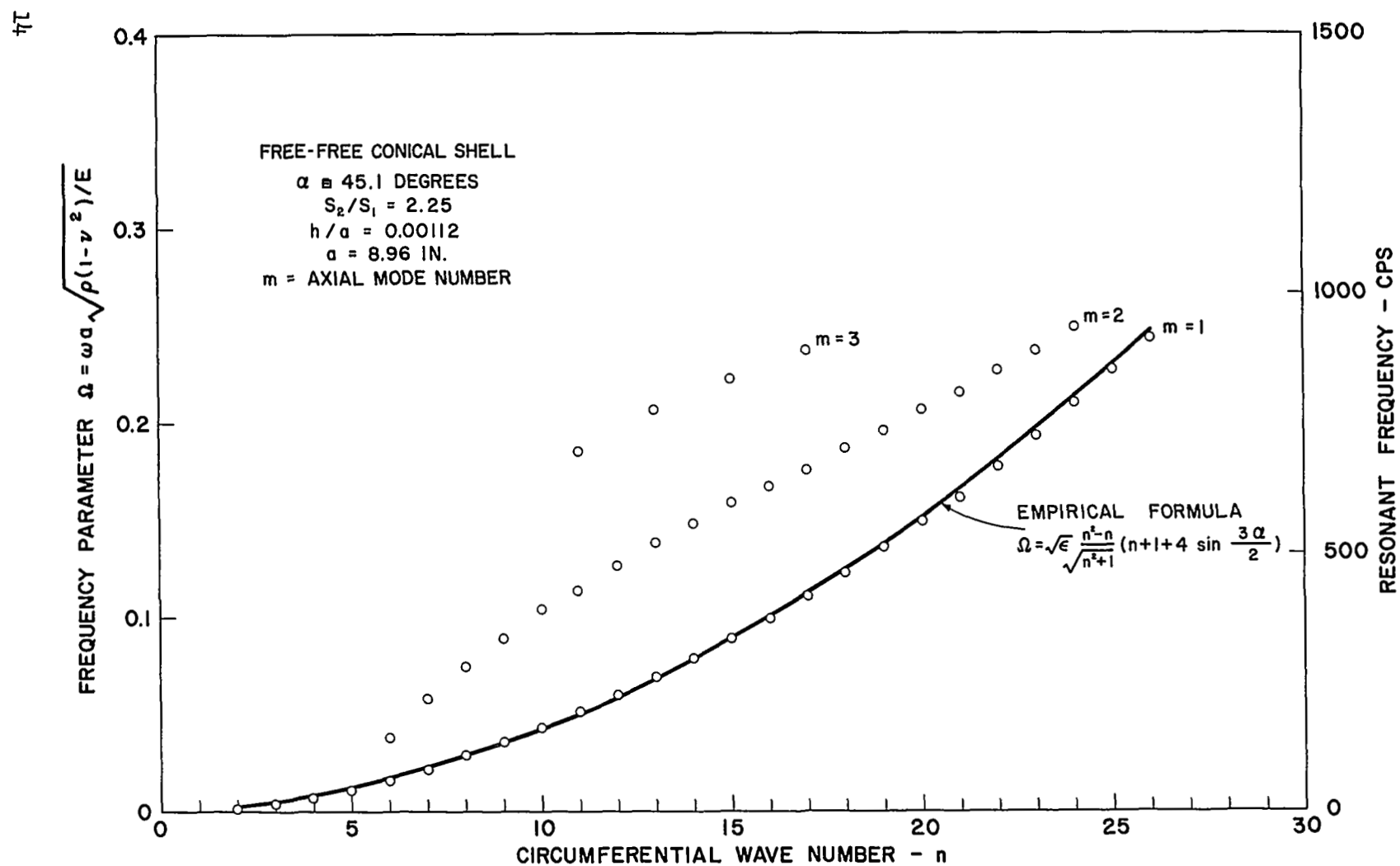
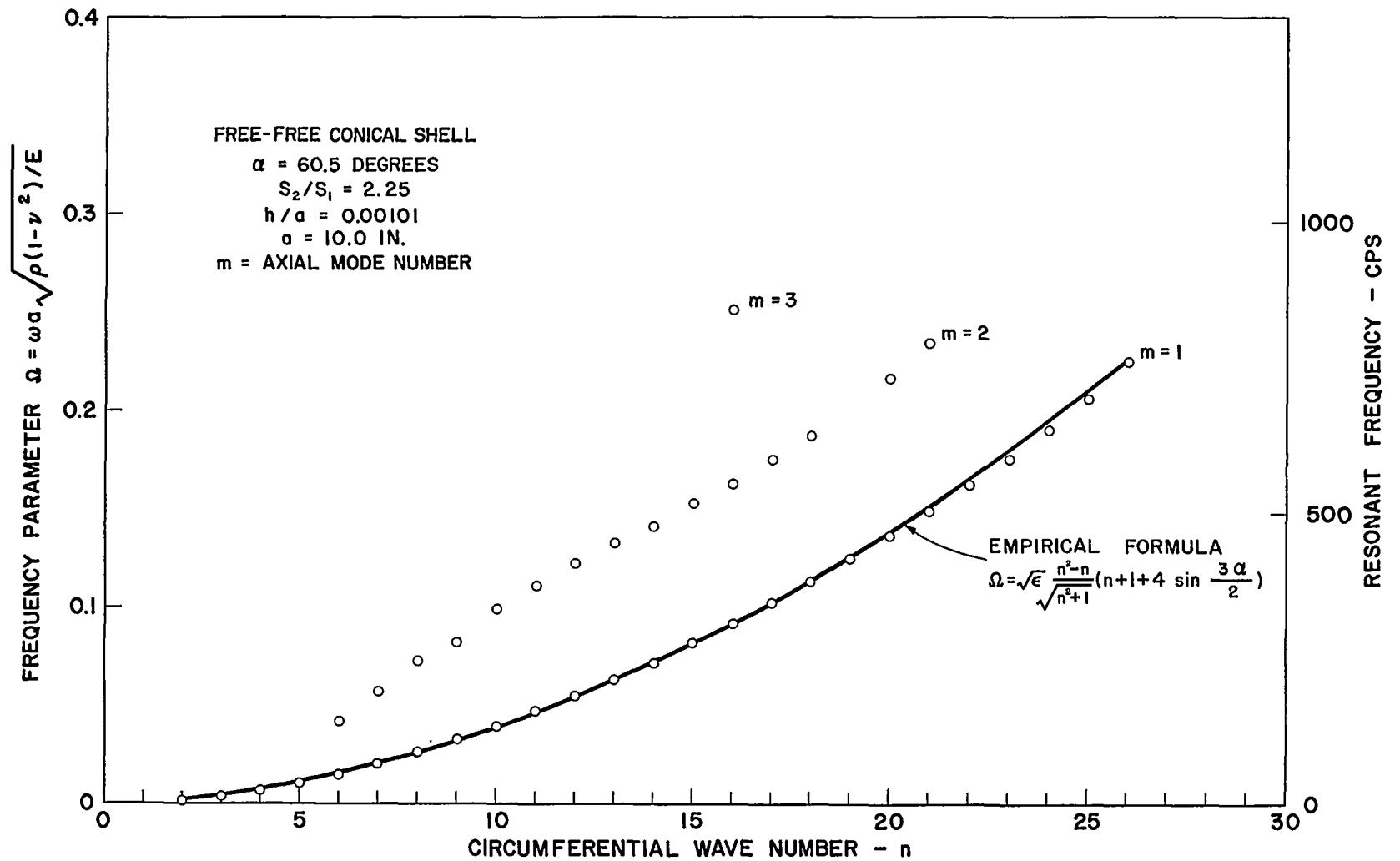


Figure 4. Resonant Frequencies for 45.1° Cone



252

Figure 5. Resonant Frequencies for 60.5° Cone

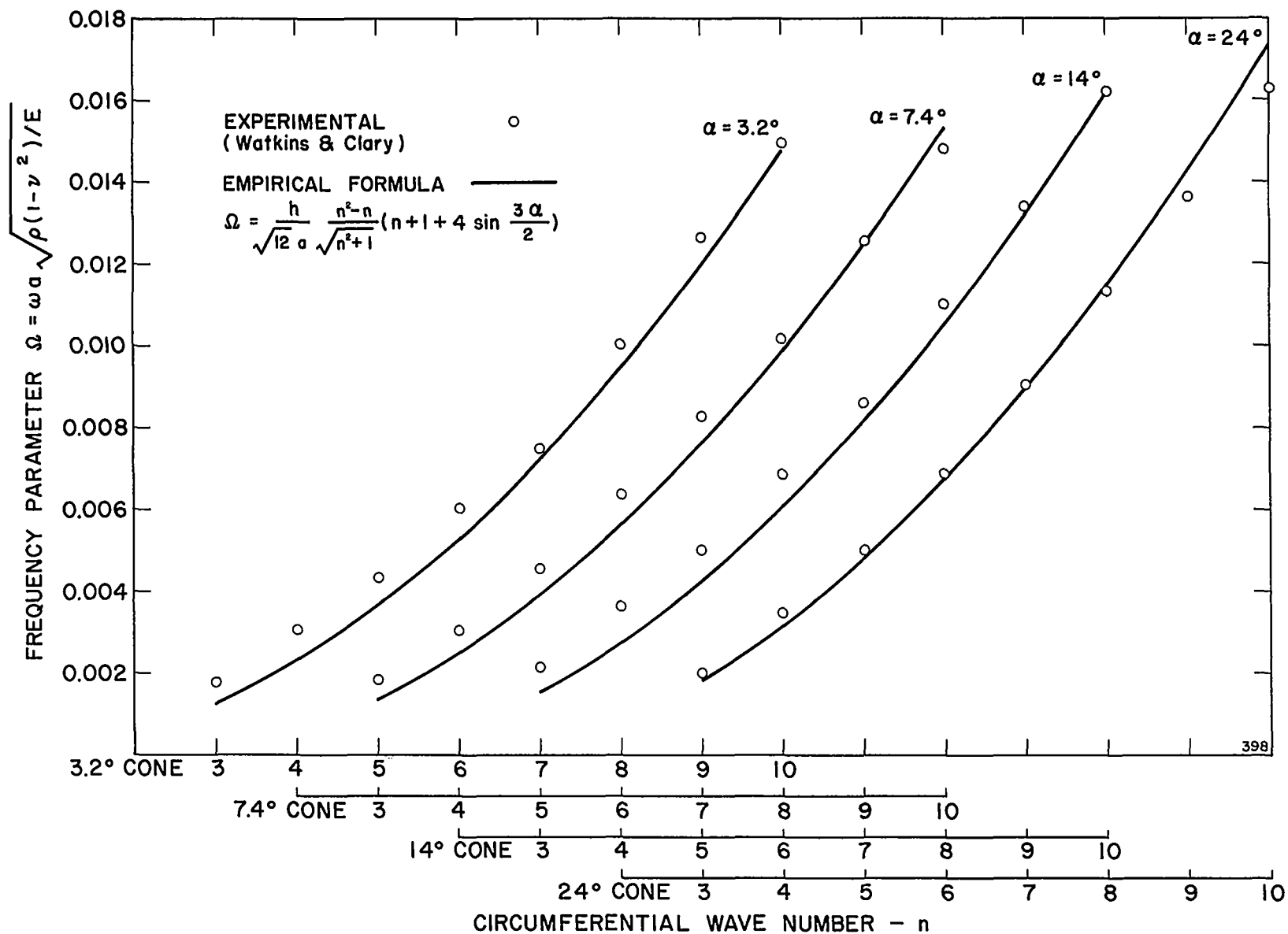


Figure 6. Correlation of Equation 2 with Experimental Data of Reference 2

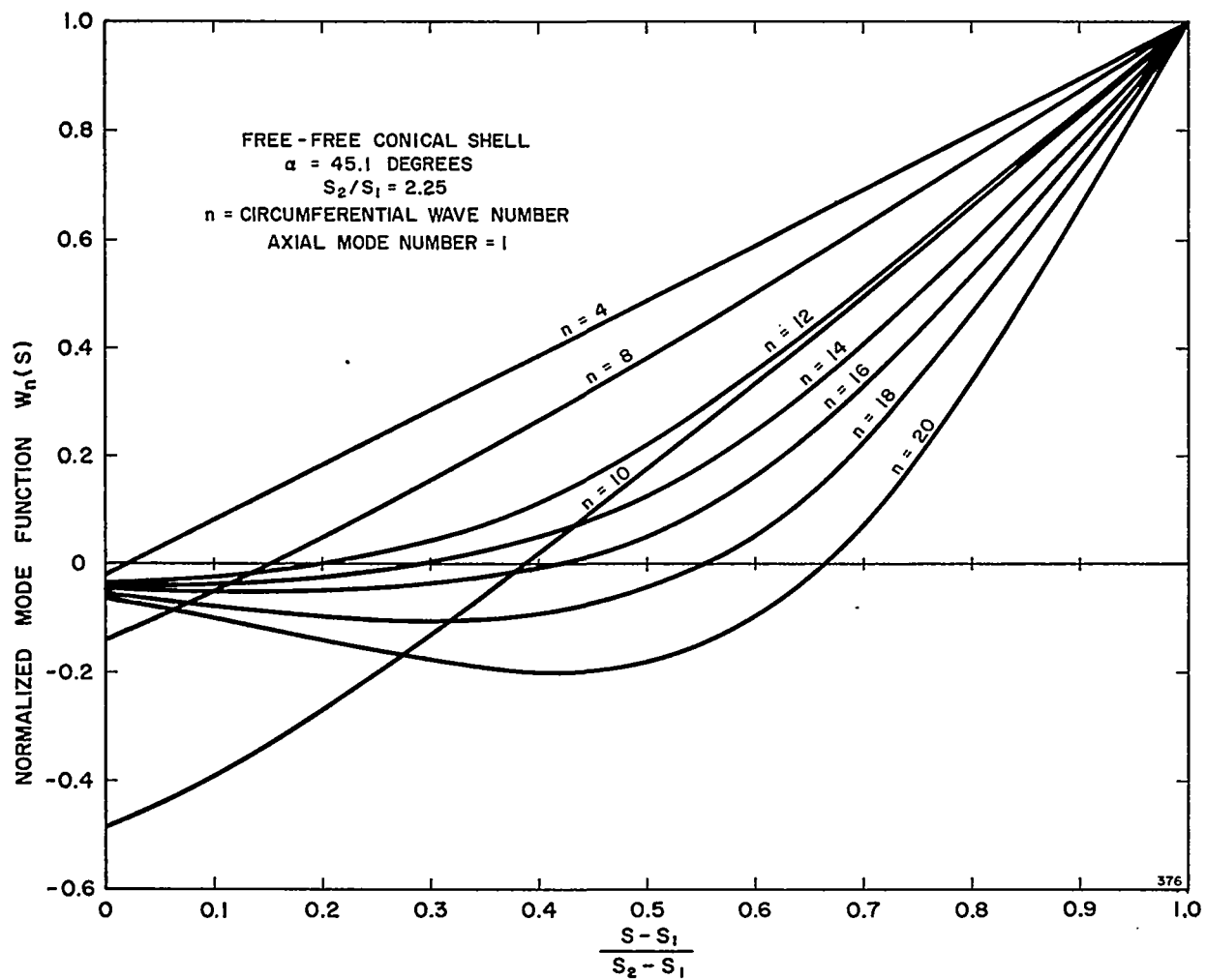


Figure 7. Mode Shapes for First Axial Mode
 ($m = 1$) for 45.1° Cone

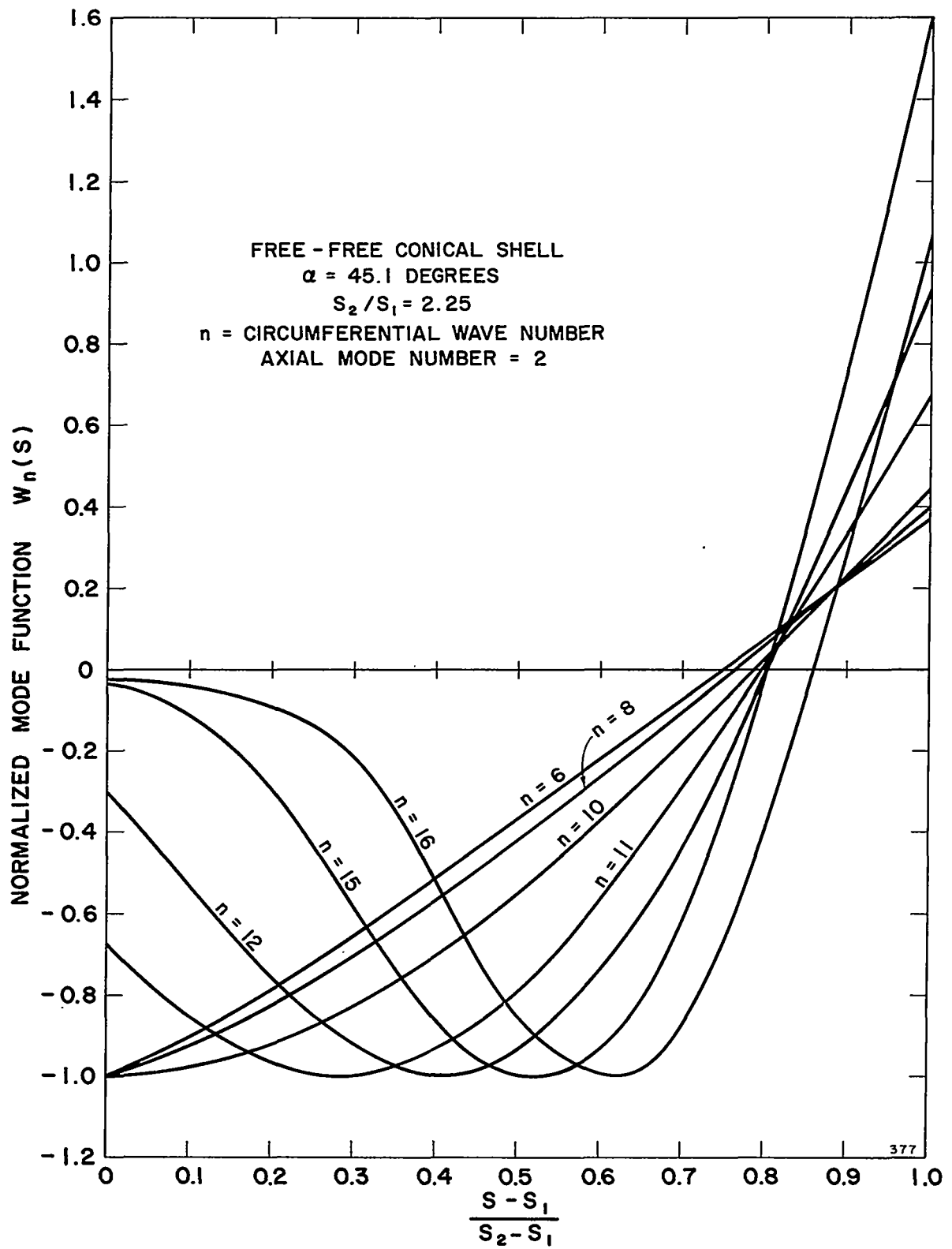


Figure 8. Mode Shapes for Second Axial Mode ($m = 2$) for 45.1° Cone

APPENDIX

Frequency Data for Free-Free Cones

Model No. 1

n	m = 1			m = 2		m = 3		m = 4	
	Experimental f (cps)	Ω	Calculated* Ω	Experimental f (cps)	Ω	Experimental f (cps)	Ω	Experimental f (cps)	Ω
2	10.6	.00191	.00191	62.4	.0113				
3	27.8	.00502	.00496	108	.0195				
4	52.4	.00945	.00901	150	.0271				
5	83.8	.0151	.0140	218	.0393				
6	120	.0216	.0200	288	.0520	527	.0951		
7	158	.0285	.0270	339	.0611				
8	200	.0361	.0348	385	.0694	644	.116		
9	246	.0444	.0437	435	.0785	684	.123		
10	298	.0538	.0535	493	.0889	735	.133	985	.178
11	359	.0648	.0644	552	.0996	795	.143	1051	.190
12	423	.0763	.0760	622	.112	861	.155	1123	.203
13	488	.0880	.0887	693	.125	944	.170	1182	.213
14	564	.102	.102	777	.140	1027	.185	1258	.227
15	638	.115	.117	865	.156				
16	717	.129	.133	959	.173				
17	812	.147	.149						
18	917	.165	.167						

* Equation (2)

Model No. 2

n	m = 1			m = 2		m = 3	
	Experimental f (cps)	Ω	Calculated* Ω	Experimental f (cps)	Ω	Experimental f (cps)	Ω
2	6.36	.00151	.00192				
3	17.8	.00422	.00476				
4	32.5	.00770	.00836				
5	51.4	.0122	.0127				
6	75.2	.0179	.0179	197	.0467		
7	102	.0242	.0237	264	.0626		
8	132	.0313	.0302	329	.0780		
9	164	.0389	.0375	388	.0920		
10	199	.0472	.0455	432	.1024		
11	234	.0555	.0542	470	.111	754	.179
12	273	.0647	.0638	508	.120	812	.192
13	315	.0746	.0740	555	.132	893	.212
14	359	.0851	.0849	602	.143	932	.221
15	407	.0964	.0966	662	.157	983	.233
16	459	.109	.109	721	.171	1032	.245
17	513	.122	.122	782	.185		
18	570	.135	.136	845	.200		
19	632	.150	.151				
20	695	.165	.166				
21	763	.181	.182				
22	829	.197	.199				

*
Equation (2)

Model No. 3

n	m = 1			m = 2		m = 3	
	Experimental f (cps)	Ω	Calculated* Ω	Experimental f (cps)	Ω	Experimental f (cps)	Ω
2	5.54	.00147	.00193				
3	15.0	.00399	.00473				
4	27.1	.00721	.00820				
5	42.4	.0113	.0124				
6	60.7	.0162	.0171	144	.0383		
7	82.0	.0218	.0225	219	.0583		
8	108	.0287	.0286	280	.0745		
9	135	.0359	.0353	334	.0889		
10	163	.0434	.0427	392	.104		
11	193	.0514	.0507	442	.118	698	.186
12	225	.0599	.0593	476	.127		
13	260	.0692	.0685	520	.138	776	.206
14	296	.0788	.0785	557	.148		
15	333	.0886	.0892	597	.159	835	.222
16	374	.0995	.100	630	.168		
17	416	.111	.112	650	.173	892	.237
18	461	.123	.125	703	.187		
19	511	.136	.138	740	.196		
20	561	.149	.152	777	.207		
21	608	.162	.166	810	.216		
22	667	.177	.182	854	.227		
23	727	.193	.197	892	.237		
24	790	.210	.214	937	.249		
25	853	.227	.231				
26	915	.244	.249				

*
Equation (2)

Model No. 4

n	m = 1			m = 2		m = 3	
	Experimental f (cps)	Calculated*		Experimental f (cps)		Experimental f (cps)	
2	4.67	.00139	.00182				
3	12.7	.00377	.00443				
4	22.9	.00680	.00765				
5	35.2	.0104	.0115				
6	50.2	.0149	.0158	142	.0422		
7	67.5	.0200	.0208	193	.0573		
8	88.9	.0264	.0264	247	.0734		
9	110	.0326	.0325	277	.0823		
10	134	.0398	.0392	336	.0998		
11	159	.0472	.0465	374	.111		
12	186	.0552	.0544	413	.123		
13	213	.0633	.0629	447	.133		
14	242	.0719	.0719	477	.142		
15	276	.0820	.0816	514	.153		
16	309	.0918	.0918	550	.163	847	.252
17	345	.102	.103	591	.175		
18	382	.113	.114	631	.187		
19	421	.125	.126				
20	460	.137	.139	730	.217		
21	502	.149	.152	790	.235		
22	547	.162	.165				
23	592	.176	.180				
24	641	.190	.194				
25	694	.206	.210				
26	758	.225	.226				

*
Equation (2)